

## Conclusion

Detailed knowledge of the membrane association of cytochrome P450s is important for understanding conformational changes, dynamic interactions with redox partners, substrate accessibility, heme topology, and aggregation. The assays described here provide a basis for ascertaining the effects of protein modification on membrane binding and, by inference, the role of specific regions of the protein in membrane interactions. These assays have implicated the region between F and G helices of P450 2C5 in membrane interactions and in the aggregation of the protein when dissociated from membranes.<sup>1</sup>

## Acknowledgment

This work is supported in part by USPHS Grant GM31001 (E.F.J.).

# [13] Sensitizer-Linked Substrates and Ligands: Ruthenium Probes of Cytochrome P450 Structure and Mechanism

By IVAN J. DMOCHOWSKI, ALEXANDER R. DUNN, JONATHAN J. WILKER,  
BRIAN R. CRANE, MICHAEL T. GREEN, JOHN H. DAWSON,  
STEPHEN G. SLIGAR, JAY R. WINKLER, and HARRY B. GRAY

## Introduction

Covalent attachment of the photosensitizer  $[\text{Ru}(\text{bpy})_3]^{2+}$  (bpy is 2,2'-bipyridine) to a substrate or ligand (Fig. 1) constitutes a powerful method for probing the steric and electronic properties of buried cytochrome P450 active sites. Researchers have exploited the versatile laser-triggered photoredox chemistry of  $[\text{Ru}(\text{bpy})_3]^{2+}$  for the rapid modulation of enzyme oxidation states.<sup>1-7</sup> Relative to conventional

<sup>1</sup> D. W. Low, J. R. Winkler, and H. B. Gray, *J. Am. Chem. Soc.* **118**, 117 (1996).

<sup>2</sup> M. J. Bjerrum, D. R. Casimiro, I.-J. Chang, A. J. DiBilio, H. B. Gray, M. G. Hill, R. Langen, G. A. Mines, L. K. Skov, J. R. Winkler, and D. S. Wuttke, *J. Bioenerget. Biomembr.* **27**, 295 (1995).

<sup>3</sup> J. Berglund, T. Pascher, J. R. Winkler, and H. B. Gray, *J. Am. Chem. Soc.* **119**, 2464 (1997).

<sup>4</sup> J. J. Wilker, I. J. Dmochowski, J. H. Dawson, J. R. Winkler, and H. B. Gray, *Angew. Chem. Int. Ed.* **38**, 90 (1999).

<sup>5</sup> I. F. Sevrioukova, C. E. Immoos, T. L. Poulos, and P. Farmer, *Israel J. Chem.* **40**, 47 (2000).

<sup>6</sup> I. Hamachi, S. Tanaka, S. Tsukiji, S. Shinkai, M. Shimizu, and T. Nagamune, *Chem. Commun.* 1735 (1997).

<sup>7</sup> I. Hamachi, S. Tanaka, S. Tsukiji, S. Shinkai, and S. Oishi, *Inorg. Chem.* **37**, 4380 (1998).

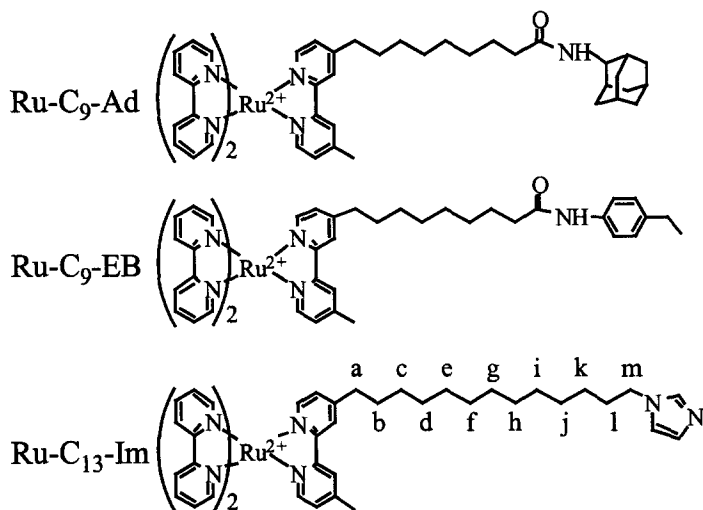


FIG. 1. Sensitizer-linked substrates (Ru-Ad, Ru-EB) and ligands (Ru-Im) for cytochromes P450. Methylens in the Ru-C<sub>13</sub>-Im alkyl chain are labeled (a–m) for purposes of NMR characterization (see Synthesis of Ru Probes).

stopped-flow methods, this photochemical approach affects oxidation and reduction over a wide range of time scales (nanosecond–millisecond) with varying thermodynamic driving forces. Ruthenium (Ru) probes can be synthesized in three to four steps from commercially available photosensitizers, linkers, and substrates; varying each component “tunes” specific binding and electronic interactions with P450.<sup>4,8,9</sup> Due to their roles in xenobiotic metabolism and steroid biosynthesis, P450s are important pharmaceutical targets. Active site-directed photosensitizers can bind both bacterial and human P450s with high affinity ( $K_D \sim 1 \mu\text{M}$ ).<sup>10</sup> Sensitizer-linked substrates target cytochromes P450 in a background of other heme enzymes, and their demonstrated biosensing and substrate screening capabilities may facilitate future drug design efforts.<sup>8,9</sup>

Unlike many structural probes of the P450 hydrophobic pocket,<sup>11</sup> sensitizer-linked substrates bind reversibly and may undergo modest turnover during biological catalysis. Resonance Raman spectroscopy interrogates the heme environment in P450  $\text{Fe}^{2+}\text{-CO}$  Ru–substrate complexes, as was shown previously with other

<sup>8</sup> I. J. Dmochowski, B. R. Crane, J. J. Wilker, J. R. Winkler, and H. B. Gray, *Proc. Natl. Acad. Sci. U.S.A.* **96**, 12987 (1999).

<sup>9</sup> I. J. Dmochowski, J. R. Winkler, and H. B. Gray, *J. Inorg. Biochem.* **81**, 221 (2000).

<sup>10</sup> A. R. Dunn, I. J. Dmochowski, C. D. Stout, J. R. Winkler, and H. B. Gray, manuscript in preparation (2002).

<sup>11</sup> P. R. Ortiz de Montellano and M. A. Correia, in “Cytochrome P450: Structure, Mechanism, and Biochemistry” (P. R. Ortiz de Montellano, ed.), 2nd Ed., p. 305. Plenum Press, New York, 1995.

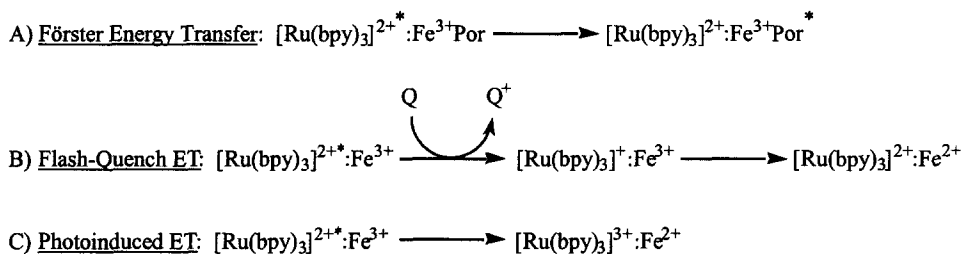


FIG. 2. Interaction of  $\text{Ru}^{2+*}$  with the P450 heme. The quencher (Q) is *p*-methoxydimethylaniline.

P450 substrates.<sup>12–15</sup> X-ray structure determination of cytochrome P450cam cocrystallized with Ru-C<sub>9</sub>-Ad identified an “open conformation” by which loop and helix movements accommodate substrates in the channel.<sup>8,16</sup>

Photoexcitation of Ru–substrate:P450 complexes, either in steady-state or in time-resolved experiments, generates the excited state,  $\text{Ru}^{2+*}$ , which can interact with the heme by a variety of energy transfer and electron transfer (ET) processes (Fig. 2). The fraction of  $\text{Ru}^{2+*}$  luminescence quenched by the enzyme shows binding constants for this class of molecules that agree with traditional measurements of spin shifts at the ferric heme. Furthermore, energy transfer kinetics from  $\text{Ru}^{2+*}$  to the heme provide a “molecular ruler” for measuring the depth of P450 channels. Indeed, Ru–Fe distances calculated by Förster analysis<sup>17</sup> are entirely consistent with crystallographic data for two different Ru–adamantyl:P450 complexes.<sup>8,16</sup> Thus, luminescence data provide detailed structural information not easily obtained by other spectroscopic methods.

Finally, Ru–substrates complement existing mechanistic probes by providing an efficient ET pathway to the P450 heme through the hydrocarbon linker. Due to rate-limiting ET ( $k \approx 50 \text{ sec}^{-1}$ ) in the natural enzymatic system (e.g., via NADH, putidaredoxin reductase, and putidaredoxin), reactive Fe-peroxy and ferryl intermediates in P450 catalytic cycles are not readily observable.<sup>18</sup> These reductant cofactors are also economically infeasible for industrial biosynthetic applications

<sup>12</sup> A. V. Wells, P. Li, and P. M. Champion, *Biochemistry* **31**, 4384 (1992).

<sup>13</sup> C. Jung, G. H. B. Hoa, K.-L. Schroeder, M. Simon, and J. P. Doucet, *Biochemistry* **31**, 12855 (1992).

<sup>14</sup> O. Bangcharoenpaupong, P. M. Champion, S. A. Martinis, and S. G. Sligar, *J. Chem. Phys.* **87**, 4273 (1987).

<sup>15</sup> T. Uno, Y. Nishimura, R. Makino, T. Iizuka, and Y. I. Tsuboi, *J. Biol. Chem.* **260**, 2023 (1985).

<sup>16</sup> A. R. Dunn, I. J. Dmochowski, A. M. Bilwes, H. B. Gray, and B. R. Crane, *Proc. Natl. Acad. Sci. U.S.A.* **98**, 12420 (2001).

<sup>17</sup> T. Förster, *Discussions Faraday Soc.* **27**, 7 (1959).

<sup>18</sup> M. J. Hintz, D. M. Mock, L. L. Peterson, K. Tuttle, and J. A. Peterson, *J. Biol. Chem.* **257**, 14324 (1982).

and remain unidentified for certain P450s.<sup>19,20</sup> The ongoing search for electrochemical and photochemical alternatives<sup>4,5,21–23</sup> has led us to develop conjugated Ru probes that mediate photoinduced ET on a nanosecond time scale (Fig. 2C).<sup>10</sup> This article describes methodologies for employing sensitizer-linked substrates and ligands as probes of P450 structure and mechanism.

## Methods

### *Enzymes, Reagents, and Ruthenium Probes*

P450, putidaredoxin reductase (PdR), and putidaredoxin (Pd) are expressed and purified with minor modifications to literature procedures,<sup>18,24–26</sup> stored at  $-70^{\circ}$ , and thawed just before use. P450 as described here is camphor-free, unless stated otherwise. Camphor is removed by eluting the enzyme at  $4^{\circ}$  on a desalting column (PD-10, 50 mM Tris-HCl, pH 7.4), followed by a second PD-10 column equilibrated with buffer A (50 mM potassium phosphate, 100 mM potassium chloride, pH 7.4). NADH (Sigma, St. Louis, MO), substrate amines (Aldrich, Milwaukee, WI), bromoalkyl linkers (Aldrich), and *cis*-[Ru(bpy)<sub>2</sub>Cl<sub>2</sub>] (Strem, Newburyport, MA) are purchased and used without further purification. The reductive quencher, *para*-methoxy-*N,N*-dimethylaniline (*p*-MDMA), is synthesized following established procedures.<sup>27,28</sup>

[Ru-C<sub>*n*</sub>-Ad]Cl<sub>2</sub> (Fig. 1) is synthesized as described previously,<sup>9</sup> where “C<sub>*n*</sub>” indicates the number of methylene units separating 2,2'-bipyridine (bpy) from adamantylamine (Ad). Ru-C<sub>9</sub>-EB (EB refers to ethyl benzene, Fig. 1) is synthesized analogously by linking 8-bromooctanoic acid to 4-ethylaniline via an amide bond.<sup>28</sup> Imidazole-terminated Ru probes (Ru-Im), through their covalent linkage to the heme, are better coupled electronically and generally bind more selectively than their substrate analogs.<sup>8</sup> We have described the synthesis of Ru-C<sub>*n*</sub>-Ad/EB/Im with various alkyl linkers ( $n = 7–13$ ).<sup>28</sup> The synthesis and binding of Ru-C<sub>13</sub>-Im (Fig. 1) are described herein.

<sup>19</sup> M. A. McLean, S. A. Maves, K. E. Weiss, S. Krepich, and S. G. Sligar, *Biochem. Biophys. Res. Commun.* **252**, 166 (1998).

<sup>20</sup> J. K. Yano, L. S. Koo, D. J. Schuller, H. Y. Li, P. R. Ortiz de Montellano, and T. L. Poulos, *J. Biol. Chem.* **275**, 31086 (2000).

<sup>21</sup> U. Schwaneberg, D. Appel, J. Schmitt, and R. D. Schmid, *J. Biotechnol.* **84**, 249 (2000).

<sup>22</sup> K. K. Lo, L.-L. Wong, and H. A. O. Hill, *FEBS Lett.* **451**, 342 (1999).

<sup>23</sup> N. Sugihara, Y. Ogoma, K. Abe, Y. Kondo, and T. Akaike, *Polymers Adv. Tech.* **9**, 307 (1998).

<sup>24</sup> C. A. Tyson, J. D. Lipscomb, and I. C. Gunsalus, *J. Biol. Chem.* **247**, 5777 (1972).

<sup>25</sup> P. W. Roome, J. C. Phillely, and J. A. Peterson, *J. Biol. Chem.* **258**, 2593 (1983).

<sup>26</sup> J. A. Peterson, M. C. Lorence, and B. Amarnah, *J. Biol. Chem.* **265**, 6066 (1989).

<sup>27</sup> N. Sekiya, M. Tomie, and N. J. Leonard, *J. Org. Chem.* **33**, 318 (1968).

<sup>28</sup> I. J. Dmochowski, “Probing Cytochrome P450 with Sensitizer-Linked Substrates.” California Institute of Technology, Pasadena, 2000.

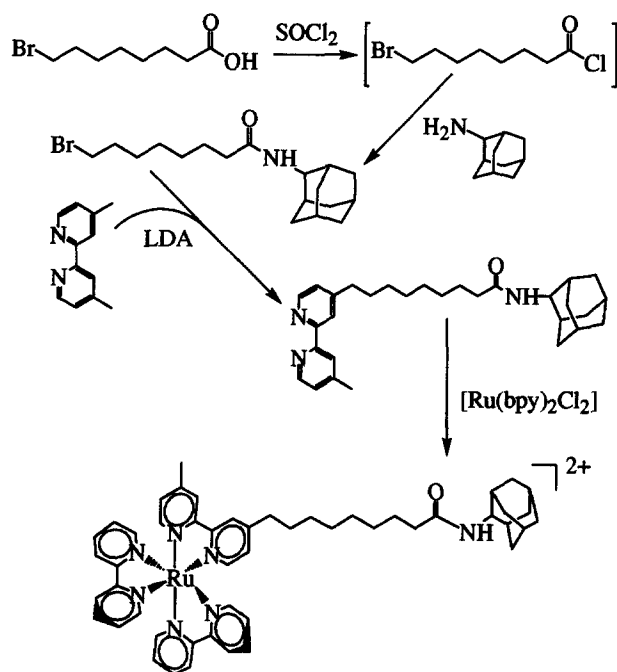


FIG. 3. Synthetic scheme for a prototypal sensitizer-linked substrate,  $[\text{Ru}-\text{C}_9-\text{Ad}]\text{Cl}_2$ .

### Synthesis of Ru Probes

A general procedure for generating sensitizer-linked substrates is outlined in Fig. 3. This protocol may be generalized to include any combination of photosensitizer, linker, and substrate/ligand that targets the desired P450 active site. We have synthesized numerous compounds: Ru and Os photosensitizers with substituted bipyridine, terpyridine, phenanthroline, and imidazole ligands; alkyl, polyethylene glycol, perfluorobiphenyl, and polyxylyl linkers; attached via amide, ether, or amino bonds to substrates (adamantane, ethyl benzene, borneol, norbornane, thioanisole styrene) or imidazole ligands. All reactions are performed under an inert atmosphere with dried and freshly distilled solvents. Nonfluorescing silica thin-layer chromatography (TLC) plates are used for monitoring bpy ligand syntheses, as bpy coordination of the metal in fluorescing plates renders the compounds stationary. TLC plates are imaged with an aqueous ferric salt solution, which turns bpy-containing spots red.

### Synthesis of $[\text{Ru}-\text{C}_{13}-\text{Im}]\text{Cl}_2$

4-(13-Bromotridecyl)-4'-methyl-[2,2']bipyridinyl(*bpy*- $\text{C}_{13}$ -Br). Diisopropylamine (0.770 g, 7.61 mmol), *n*-butyllithium (7.60 mmol in hexanes), and

tetrahydrofuran (THF, 10 ml) are combined in a Schlenk flask chilled over an ice bath. A cold solution of 4,4'-dimethyl-2,2'-bipyridine (1.40 g, 7.60 mmol) in 40 ml of THF is added by cannula over 15 min. To this solution is added 1,12-dibromododecane (25.0 g, 76.2 mmol) in THF (20 ml). The reaction is stirred on ice for 3 hr and is then allowed to warm to room temperature for further stirring overnight. The solution is transferred to a separatory funnel to which water (15 ml) and ether (15 ml) are added. The organic layer is washed with saturated  $\text{NaHCO}_3$ , dried with  $\text{MgSO}_4$ , and evaporated to a beige solid under vacuum. Silica gel column chromatography with  $\text{CHCl}_3$  as the eluent yields 1.31 g (40.0%) of a white solid.  $^1\text{H NMR}$  ( $\text{CDCl}_3$ ):  $\delta \sim 1.7$  (m,  $\text{CH}_{2\text{c-k}}$ ), 1.75 (p,  $\text{CH}_{2\text{b}}$ ), 1.85 (p,  $\text{CH}_{2\text{l}}$ ), 2.55 (s, bpy- $\text{CH}_3$ ), 2.76 (t, bpy- $\text{CH}_2$ ), 3.48 (t,  $\text{CH}_2$ -Br), 7.26 (d, bpy 5 and 5'), 8.40 (d, bpy 3 and 3'), 8.65 (t, bpy 6 and 6').

4-(13-Imidazol-1-yl-tridecyl)-4'-methyl-[2,2']bipyridinyl (bpy- $\text{C}_{13}$ -Im). Imidazole (1.0 g, 15 mmol) and bpy- $\text{C}_{13}$ -Br (0.30 g, 0.70 mmol) are combined in a flask with THF (50 ml) and refluxed for 4 days. The solvent is removed under vacuum, and the resulting solid is dissolved in  $\text{CHCl}_3$  for washing by saturated  $\text{NaHCO}_3$ , water, and NaCl. The product is purified by silica gel column chromatography using ethyl acetate as the eluent to yield 0.26 g (90%) of a white solid.  $^1\text{H NMR}$  ( $\text{CDCl}_3$ ):  $\delta \sim 1.3$  (m,  $\text{CH}_{2\text{c-k}}$ ), 1.71 (p,  $\text{CH}_{2\text{b}}$ ), 1.76 (p,  $\text{CH}_{2\text{l}}$ ), 2.42 (s, bpy- $\text{CH}_3$ ), 2.73 (t, bpy- $\text{CH}_2$ ), 3.95 (t,  $\text{CH}_{2\text{m}}$ ), 6.90 (s, imid H-5), 7.10 (s, imid H-4), 7.19 (d, bpy 5 and 5'), 7.68 (s, imid H-2), 8.24 (s, bpy 3 and 3'), 8.60 (t, bpy 6 and 6').

$[\text{Ru}(\text{bpy})_2(\text{bpy-}\text{C}_{13}\text{-Im})]\text{Cl}_2$ . The ligand bpy- $\text{C}_{13}$ -Im (460 mg, 1.10 mmol) and *cis*- $[\text{Ru}(\text{bpy})_2\text{Cl}_2]$  (538.6 mg, 1.04 mmol) are combined with 5:1 (v/v) water/ethanol (18 ml) and refluxed for 12 hr. The solvent is removed under vacuum, and the dark red solid is dissolved in water (60 ml). This aqueous solution is combined with a solution of  $\text{NH}_4\text{PF}_6$  (1.20 g, 7.36 mmol) in water (20 ml) to yield an orange precipitate. The aqueous slurry is extracted with  $\text{CH}_2\text{Cl}_2$  (75 ml); the organic layer is washed with 0.01 M HCl ( $2 \times 50$  ml), 0.01 M NaOH ( $2 \times 50$  ml), and water ( $2 \times 75$  ml) prior to rotary evaporation. The  $\text{PF}_6^-$  salt of this ruthenium complex is purified by silica gel flash chromatography employing an eluent of 3% (v/v) methanol in  $\text{CH}_2\text{Cl}_2$ . Pure fractions are combined and dried by rotary evaporation. In order to metathesize the ruthenium complex to the  $\text{Cl}^-$  salt, the purified  $\text{PF}_6^-$  salt is dissolved in methanol (10 ml) and loaded onto a CM Sepharose cation-exchange column ( $2 \times 13$  cm). The column is washed with water (600 ml), and the ruthenium complex is then eluted with 500 mM NaCl (300 ml) and dried by vacuum. The desired  $[\text{Ru}(\text{bpy})_2(\text{bpy-}\text{C}_{13}\text{-Im})]\text{Cl}_2$  is isolated from the NaCl-containing solid by repeated extractions with  $\text{CH}_2\text{Cl}_2$ , followed by filtering and drying under vacuum. Yield of the dark red solid is 188 mg (20.0%).  $^1\text{H NMR}$  ( $\text{CD}_2\text{Cl}_2$ ):  $\delta \sim 1.3$  (m,  $\text{CH}_{2\text{c-k}}$ ), 1.72 ( $\text{CH}_{2\text{b,l}}$ ), 2.60 (s, bpy'- $\text{CH}_3$ ), 2.85 (t, bpy'- $\text{CH}_2$ ), 3.99 (t,  $\text{CH}_{2\text{m}}$ ), 7.04 (m), 7.26 (m), 7.48 (m), 7.71 (m), 8.13 (m), 8.63 (s), 8.70 (s), 9.07 (m). LRMS (electrospray, positive ion) calcd for  $\text{C}_{47}\text{H}_{54}\text{N}_8\text{Ru}$  ( $\text{M} + \text{H}^+$ )  $m/z$  833, found 833.

### *Transient Absorbance and Time-Resolved Luminescence Spectroscopic Methods*

Solution experiments are performed in sealed cuvettes with equimolar P450 (camphor-free) and Ru-probe (5–10  $\mu\text{M}$ ) in buffer A. Flash-quench experiments also include the reductive quencher *p*-MDMA at concentrations (5–10 mM) sufficient for efficient Ru<sup>2+</sup> quenching. Cuvettes are fitted with a magnetic stir bar and are deoxygenated by repeated evacuations on a vacuum line, followed by backfilling with purified argon (three rounds of 10 cycles).

All samples are excited with a tunable (220–2000 nm, excitation at 480 nm) optical parametric oscillator (Spectra Physics, Mountain View, CA, MOPO) pumped by a frequency-tripled Q-switched Nd:YAG laser (Spectra Physics, 355 nm, 350 mJ/pulse, 8 ns FWHM). The YAG fires continuously at 10 Hz; thus, for longer time base experiments (>50 ms), software was written to select pulses with a shutter. The laser output is attenuated with a polarizer to give a 1- to 2-mJ/pulse at the sample. Laser shots with energies differing by more than 10% from the mean value (laser pulses detected by a photodiode and selected by a discriminator, Phillips Scientific Model 6930) are rejected.

Kinetics data are collected as averages of at least 250 laser shots.<sup>28</sup> Transient absorption traces are typically fit to mono- or biexponential functions ( $y = c_0 + c_1 e^{-(k_{\text{en}} + k_0)t} + c_2 e^{-k_0 t}$ ) using a least-squares fitting routine. Luminescence decay data are fit similarly, but must be deconvolved from the instrument response function ( $\sim 10$  ns FWHM) in cases where Ru<sup>2+</sup> luminescence is highly quenched by the protein ( $\tau < 50$  ns).

### *Resonance Raman Spectroscopy of P450 Fe<sup>2+</sup>-CO Substrate Complexes*

Samples (200  $\mu\text{l}$ , 100  $\mu\text{M}$  P450 in buffer A, substrate concentration, 1 mM) are prepared in quartz NMR tubes sealed with a rubber septum. The solutions are bubbled gently with carbon monoxide for several minutes before adding a spatula tip of dithionite ( $\sim 1$  mg). Formation of the Fe<sup>2+</sup>-CO complex is verified by UV-Vis ( $\lambda_{\text{max}} = 446$  nm) and reconfirmed after each experiment. Samples are excited at 441 nm with a HeCd laser (Liconix (Santa Clara, CA) Model 424ONB, 40 mW), and Raman scatter is focused using longitudinal and transverse collection optics onto a double spectrometer (SPEX 1403, 0.85 m) interfaced to a PC via the SPEX MSD2 module. The signal is collected using a PMT (Hamamatsu R955, Hamamatsu City, Japan) biased at  $-1100$  V (Pacific Precision Instruments, San Diego, CA). The sample control unit, photon counter, amplifier/discriminator, and buffered interface are all from EG&G Instruments (Gaithersburg, MD).

### *Catalytic Oxidation of [Ru-C<sub>9</sub>-Ad]Cl<sub>2</sub> with NADH/PdR/Pd/P450*

All reagents (NADH, PdR, Pd, P450) are tested prior to use by measuring NADH consumption in the presence of camphor: our finding of  $575 \pm 25$   $\mu\text{mol}$  NADH/min/ $\mu\text{mol}$  P450 agrees with literature values.<sup>29</sup>

<sup>29</sup> J. J. De Voss and P. R. Ortiz de Montellano, *J. Am. Chem. Soc.* **117**, 4185 (1995).

A 1.5-ml solution in buffer A containing 1  $\mu\text{M}$  P450, 1  $\mu\text{M}$  PdR, 10  $\mu\text{M}$  Pd, 10  $\mu\text{M}$  [Ru-C<sub>9</sub>-Ad]Cl<sub>2</sub>, and 200  $\mu\text{M}$  NADH ( $\epsilon = 6.22 \text{ mM}^{-1}\text{cm}^{-1}$  at 340 nm)<sup>18</sup> is put in a cuvette. The solution is maintained at 20° and is mixed continuously (500 rpm) with a Hewlett Packard (Palo Alto, CA) 89090A stirrer/temperature controller. The consumption of NADH is monitored at 340 nm for 4 min (at 2-sec intervals) using the kinetics software package on a PC-controlled Hewlett Packard 8452A spectrophotometer.

Aliquots (250  $\mu\text{l}$ ) are removed 1, 2, and 3 min after the addition of P450 and are quenched immediately with a 1-*M* ethanolic camphor solution (final camphor concentration, 2 *M*). Camphor displaces Ru substrates from the P450 pocket, and the enzyme consumes leftover NADH rapidly. The remaining reaction volume (~750  $\mu\text{l}$ ) is quenched with camphor after 4 min. Water (3 ml) and CH<sub>2</sub>Cl<sub>2</sub> (3 ml) are added to each aliquot and shaken in a small separatory funnel. Improved separation of organic and aqueous layers is achieved by leaving the mixture at -20° overnight. The CH<sub>2</sub>Cl<sub>2</sub> layer (containing all ruthenated species, and minimal buffer salt) is isolated and evaporated to dryness. The Ru complex is redissolved in minimal methanol, and the concentration is checked by UV-Vis ( $\epsilon = 14.5 \text{ mM}^{-1}\text{cm}^{-1}$  at 456 nm).<sup>30</sup>

#### *Electrospray Ionization (ESI) Mass Spectroscopy to Monitor Product Formation*

Ru samples (~10  $\mu\text{M}$  in methanol) are injected with a 250- $\mu\text{l}$  Hamilton syringe into a LcQ (Finnigan Mat, Bremen, Germany) quadrupole ion trap mass spectrometer at a rate of 5  $\mu\text{l}/\text{min}$ ; typical runs require less than 100  $\mu\text{l}$  per sample, and data sets are averaged for 100 scans. Only positive ions are detected, and sensitivity is highest in the selected ion monitoring (SIM) mode, with a mass range of 420–460. The isotope patterns of both starting and product materials are checked against expected values. The peak spacings ( $m/z = 0.5$ ) are particularly diagnostic for these divalent species. The observation of a product ( $m/z = 445$ ) with a mass 16 units higher ( $z = +2$ ;  $m/z = 16/2$ ) than the starting material ( $m/z = 437$ ) is consistent with one or more singly hydroxylated adamantyl species, [Ru-C<sub>9</sub>-Ad-OH]Cl<sub>2</sub>.

#### *Calibration of ESI for Ratiometric Analysis of Product Yields*

A stock solution of [Ru-C<sub>9</sub>-Ad-OH]Cl<sub>2</sub> is obtained by scaling the catalytic oxidation procedure 10-fold and continuing until NADH is consumed entirely. The resulting product is diluted in acetonitrile, and its purity is confirmed by ESI mass spectroscopy. Stock solutions (10  $\mu\text{M}$ ) of [Ru-C<sub>9</sub>-Ad]Cl<sub>2</sub> and [Ru-C<sub>9</sub>-Ad-OH]Cl<sub>2</sub> in methanol are combined in proportions varying from 10 : 1 to 1 : 4. Each solution is injected three different times, with intermediary blank runs of 1 : 1 (v/v) acetonitrile : methanol. Relative peak intensities are determined using

<sup>30</sup> K. Kalyanasundaram, "Photochemistry of Polypyridine and Porphyrin Complexes." Academic Press, London, 1992.

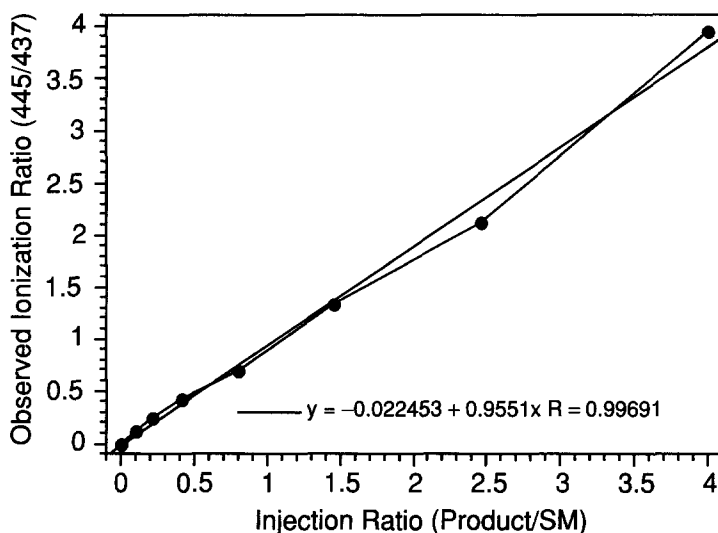


FIG. 4. Calibration line showing the relationship between the injected ratio of  $[\text{Ru-C}_9\text{-Ad-OH}]^{2+}/[\text{Ru-C}_9\text{-Ad}]^{2+}$  to the relative ionization intensity of product and starting material (SM) cations in the ESI.

standard LcQ analysis software. A calibration graph (Fig. 4) is generated from these data showing that the ionization efficiencies of Ru-C<sub>9</sub>-Ad and Ru-C<sub>9</sub>-Ad-OH are indistinguishable within experimental error (slope of 0.96). Thus, for this Ru substrate, turnover efficiency may be analyzed by directly taking the ratio of the peaks, Ru-C<sub>9</sub>-Ad-OH/Ru-C<sub>9</sub>-Ad.

## Results

### *Ru Probe Binding Monitored by UV-Vis and Time-Resolved Luminescence Measurements*

The stoichiometric addition of Ru-C<sub>9</sub>-Ad to P450 induces modest low-to-high spin conversion, as shown by a blue-shifted Soret (417 → 414 nm) and increased absorption at 392 nm (Fig. 5). Ru-C<sub>9</sub>-EB barely perturbs the Soret of six-coordinate Fe<sup>3+</sup>-OH<sub>2</sub> P450, much like the substrate ethyl benzene.<sup>31</sup> Binding of Ru-C<sub>13</sub>-Im to ferric P450 induces a small red shift (417 → 420 nm, Fig. 5). The larger spectral changes observed for the binding of imidazole itself (7 nm red shift) suggest competition between aquo and Ru-Im ligands for Fe<sup>3+</sup> P450. Full

<sup>31</sup> P. J. Loida and S. G. Sligar, *Prot. Eng.* **2**, 207 (1993).

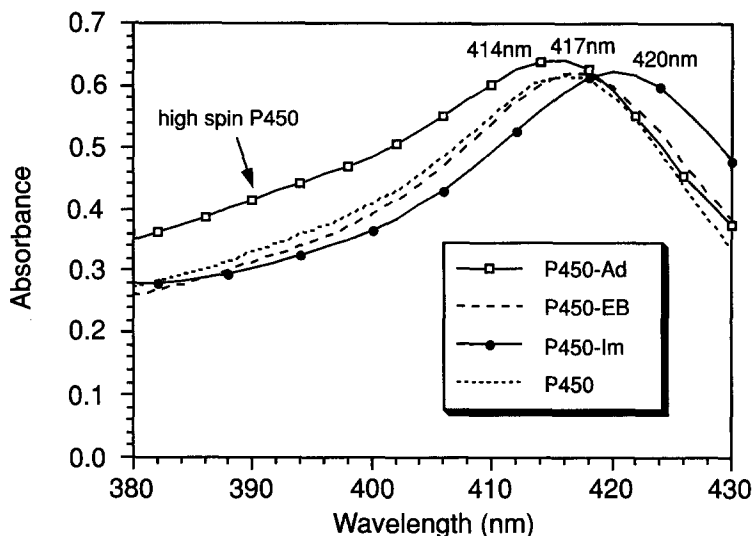


FIG. 5. UV-Vis spectra showing P450 alone ( $5.3 \mu\text{M}$ ) and in the presence of stoichiometric Ru-C<sub>9</sub>-Ad, Ru-C<sub>9</sub>-EB, and Ru-C<sub>13</sub>-Im. Solutions are buffered ( $50 \text{ mM}$  potassium phosphate,  $100 \text{ mM}$  potassium chloride, pH 7.4).

heme ligation ( $\text{Ru-Im-Fe}^{2+}$ ) accompanies reduction with dithionite (Soret shifts completely to  $446 \text{ nm}$ , as seen for P450 ferrous imidazole species).<sup>32</sup> P450<sub>cam</sub> shows tremendous selectivity for Ru-C<sub>13</sub>-Im over Ru-C<sub>11</sub>-Im<sup>8</sup>; thus, by attaching linkers with varying steric and electronic properties to the imidazole ligand,<sup>28</sup> it should be possible to engineer Ru-Im probes with considerable isozyme specificity.

Apparent dissociation constants for Ru probes are determined quickly and accurately from time-resolved luminescence measurements. Laser excitation of Ru-C<sub>13</sub>-Im in the presence of equimolar ( $10 \mu\text{M}$ ) P450 produces biphasic luminescence (60% of  $\text{Ru}^{2+}$  decays by a rapid process, Fig. 6).  $\text{Ru}^{2+}$  quenching has been shown by competition experiments with camphor to correlate directly with Ru probe binding at the active site.<sup>9</sup> Because  $[\text{Ru}]_{\text{total}} = [\text{Ru}]_{\text{quenched}} + [\text{Ru}]_{\text{free}}$ , and  $[\text{Ru}]_{\text{free}} = [\text{P450}]_{\text{free}}$ , the apparent dissociation constant for Ru-C<sub>13</sub>-Im is

$$K_D(\text{app}) = [\text{Ru}]_{\text{free}}^2 / [\text{Ru}]_{\text{bound}} = [4 \mu\text{M}]^2 / [6 \mu\text{M}] \approx 2.7 \mu\text{M} \quad (1)$$

$K_D(\text{app})$  depends somewhat on the concentrations of Ru and P450 due to competition between  $\Lambda$  and  $\Delta$  Ru stereoisomers in the racemic mixture.<sup>9</sup>

<sup>32</sup> J. H. Dawson, L. A. Andersson, and M. Sono, *J. Biol. Chem.* **258**, 13637 (1983).

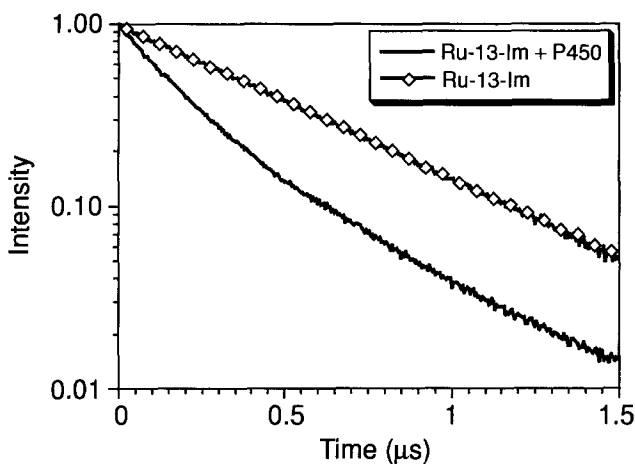


FIG. 6. Time-resolved luminescence traces showing  $[\text{Ru-C}_{13}\text{-Im}]^{2+*}$  alone (diamonds, monophasic decay,  $k_0 = 2 \times 10^6 \text{ s}^{-1}$ ) and in the presence of stoichiometric ( $5 \mu\text{M}$ )  $\text{P450}_{\text{cam}}$  (biphasic decay,  $k_{\text{en}} = 5 \times 10^6 \text{ s}^{-1}$ ,  $k_0 = 2 \times 10^6 \text{ s}^{-1}$ ).

#### Rapid Flash-Quench Photoreduction of P450 by Ru-C<sub>13</sub>-Im

Photoexcitation of P450:Ru probe complexes in the presence of *p*-MDMA leads to  $[\text{Ru-probe}]^+$  formation, followed by heme reduction on a microsecond time scale. This flash-quench scheme (Fig. 2C) has been applied to Ru-Ad, Ru-EB, and Ru-Im and promotes electron injection ( $k \sim 2 \times 10^4 \text{ s}^{-1}$ ) at rates three orders of magnitude faster than putidaredoxin. Rapid formation of  $\text{Ru-C}_{13}\text{-Im-Fe}^{2+}$  P450 is indicated by an absorbance increase at 445 nm and a decrease of the ferric Soret at 420 nm (Fig. 7), in agreement with the spectra of well-characterized P450 ferrous-imidazole species.<sup>32</sup>

#### Resonance Raman Spectra of P450 Fe<sup>2+</sup>-CO:Substrate Complexes

As shown in Table I, and as was reported previously,<sup>12-15</sup> the  $\text{Fe}^{2+}\text{-CO}$  ( $\nu_{\text{Fe-C}}$ ) stretching mode in the P450-carbon monoxide complex is quite sensitive to the nature of the substrate. These results suggest a direct interaction between bound CO and the substrate and agree with IR absorption data.<sup>33</sup> Camphor-bound  $\text{Fe}^{2+}\text{-CO}$  P450 has  $\nu_{\text{CO}} \sim 1940 \text{ cm}^{-1}$ , and camphor-free  $\text{Fe}^{2+}\text{-CO}$  P450 has two bands ( $\sim 1942$  and  $1963 \text{ cm}^{-1}$ ) that have been assigned to bent and linear structures, respectively.<sup>33</sup> The  $\nu_{\text{Fe-C}}$  stretching frequency differs by  $4 \text{ cm}^{-1}$  in the

<sup>33</sup> D. H. O'Keefe, R. E. Ebel, J. A. Peterson, J. C. Maxwell, and W. S. Caughey, *Biochemistry* **17**, 5845 (1978).

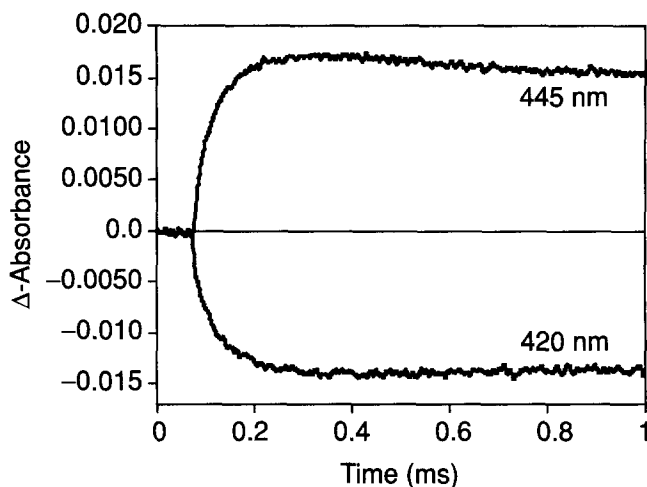


FIG. 7. Single-wavelength transient absorption:  $\Delta$ -absorbance versus time plots for the reaction of  $[\text{Ru-Im}]^+$  with P450. Changes in the Soret region (bleach of  $\text{Fe}^{3+}\text{-Im}$  at 420 nm and increase at 445 nm) are observed after laser excitation of a  $10 \mu\text{M}$  P450,  $10 \mu\text{M}$  Ru-C<sub>13</sub>-Im, 10 mM *p*-MDMA sample.

series Ru-C<sub>11</sub>-Ad, Ru-C<sub>9</sub>-Ad, and adamantane, suggesting that these substrates bind with slightly increasing proximity to the heme (Table I). These frequencies ( $472\text{--}476 \text{ cm}^{-1}$ ) lie between those found for substrate-free and camphor-bound P450 and likely reflect subtle differences in solvation and hydrogen bonding at the active site.<sup>33</sup> The similarity between binding modes for Ru-Ad compounds

TABLE I  
SUBSTRATE-INDUCED PERTURBATION OF P450 Fe-CO  
( $\nu_{\text{Fe-C}}$ ) STRETCHING FREQUENCY

Substrate	$\nu_{\text{Fe-C}}^a$
None	463 <sup>b</sup>
Ru-C <sub>11</sub> -Ad	472
Ru-C <sub>9</sub> -Ad	474
Adamantane	476
Camphor	482 <sup>b</sup>

<sup>a</sup> All units are  $\text{cm}^{-1}$ .

<sup>b</sup> These values are in good agreement with published values for substrate-free ( $465 \text{ cm}^{-1}$ ) and camphor-bound P450 ( $484 \text{ cm}^{-1}$ ). From A. V. Wells, P. Li, and P. M. Champion, *Biochemistry* **31**, 4384 (1992).



of Ru-C<sub>9</sub>-Ad. In a control experiment with NADH/PdR/Pd and no P450, the rate was found to be only 1  $\mu\text{mol NADH}/\text{min}$ ; thus, most of the observed NADH decay may be attributed to P450-mediated catalysis.

To probe the effect of linker and  $[\text{Ru}(\text{bpy})_3]^{2+}$  moieties on binding and turnover, the rate of 2-adamantylacetamide<sup>28</sup> hydroxylation was measured and found to be  $90 \pm 10 \mu\text{mol NADH}/\text{min}/\mu\text{mol P450}$ , in good agreement with the literature value for 1-adamantylacetamide ( $\sim 110 \mu\text{mol NADH}/\text{min}/\mu\text{mol P450}$ ).<sup>29</sup> Slower hydroxylation of Ru-C<sub>9</sub>-Ad can largely be attributed to differences in water displacement from the heme (95% high-spin conversion for 2-adamantylacetamide versus 25% for Ru-C<sub>9</sub>-Ad), as the biological delivery of electrons to low-spin P450<sub>cam</sub> is thermodynamically disfavored.

## Acknowledgments

This work was supported by the National Institutes of Health Metalloprotein Program Project Grant P01 GM48495, the National Science Foundation, and NIH GM 54383 (J.H.D.). I.J.D. was a NIH predoctoral trainee (GM08346), A.R.D. is a Fannie and John Hertz Graduate Fellow, B.R.C. was a Helen Hay Whitney Postdoctoral Fellow, and M.T.G. is a Burroughs-Wellcome and NIH Postdoctoral Fellow. Special thanks go to the Beckman Institute Laser and Mass Spectrometry Resource Centers at the California Institute of Technology.

## [14] Combining Pharmacophore and Protein Modeling to Predict CYP450 Inhibitors and Substrates

By COLLEN M. MASIMIREMBWA, MARIANNE RIDDERSTRÖM,  
ISMAEL ZAMORA, and TOMMY B. ANDERSSON

### Introduction

The interest in computational methods to understand the properties of cytochrome P450 (CYPs) enzymes combined with factors governing the selectivity of substrates and inhibitors for each enzyme has increased considerably over the past few years due to the development of computational methods, graphical representation, and the crystallization of a mammalian CYP enzyme. CYP enzymes are a major drug-metabolizing system, and the pharmaceutical industry has started to appreciate the potential to be able to predict metabolic properties of drugs, i.e., to virtually screen compound libraries or only to synthesize compounds with desirable metabolic properties. This chapter summarizes our experience in homology modeling of CYPs 2C8, 2C9, 2C18, and CYP2C19 based on the rabbit CYP2C5 crystal structure. A substrate selectivity analysis for the CYP2C subfamily is also